Supplementary material for

Investigation of *Abortiporus biennis* lignocellulolytic toolbox; the role of laccases in polystyrene degradation.

Anastasia Zerva[1], Romanos Siaperas[1], George Taxeidis[1], Maria Kyriakidi[1], Stamatina Vouyiouka[3], Georgios I. Zervakis[2], Evangelos Topakas[1*]

[1]*Biotechnology Laboratory, School of Chemical Engineering, National Technical University of Athens, 5 Iroon Polytechniou Str., Zografou Campus, Athens 15780, Greece*

[2]*Agricultural University of Athens, Laboratory of General and Agricultural Microbiology, Iera Odos 75, 11855 Athens, Greece*

[3]*Laboratory of Polymer Technology, School of Chemical Engineering, National Technical University of Athens, Athens, Greece*

*Correspondence: E. Topakas. Tel: +30-210-7723264; fax: +30-210-7723163; e-mail: vtopakas@chemeng.ntua.gr

Text S1

1.1 *Enzyme activities*

Cellulase and endoxylanase activities were measured as previously described (Zerva et al., 2014), using carboxymethyl cellulose (CMC) (Sigma-Aldrich, U.S.A.), or birchwood xylan (Megazyme, Ireland) as substrates. The reducing sugars were determined with the respective assay (Miller, 1959), against a suitable calibration curve.

Total esterase activity was measured with *p*-nitrophenyl- acetate (pNPA) as the substrate. pNPA was added at a final concentration of 0.5 mM to the reaction, together with 100 mM phosphate buffer, pH 6 and 20 μL enzyme sample. The mixture was incubated for 20 min in 35 ^{o}C. Free *p*-nitrophenol was determined by reading the absorbance at 410 nm.

Laccase activity was measured against 2,2′-azino-bis(3-ethylbenzthiazoline-6-sulfonic acid) (ABTS), as described in (Zerva et al., 2019). Laccase activity was also measured with catechol as substrate, under the same conditions (Zerva et al., 2019). Glucuronoyl esterase activity was determined with a commercial kit (K-GEUX3, Megazyme, Ireland), following the manufacturer's instructions.

Acetyl xylan esterase activity was measured against partially acetylated birchwood xylan (Megazyme, Ireland), at a final concentration of 0.5 % (w/v), in MOPS buffer pH 6, 100 mM. The reaction was incubated at 40 ^{o}C for 3h, and then the samples were boiled and analyzed with HPLC. The released acetic acid was quantified, in a LC-20AD system (Shimadzu) equipped with a RID-10A detector. The separation was performed on an Aminex-HPX-87H column (BioRad), with 0.3 g L^{-1} H_2SO_4 eluent at a 0.6 mL min^{-1}, for a total of 30 min analysis. The column temperature was set at 50 ^{o}C, and the injection volume was 5 μL.

α-Arabinofuranosidase activity was measured using 0.5% (w/v) wheat arabinoxylan (Megazyme, Ireland) as substrate in MOPS buffer pH 6, 100 mM. The reaction was

incubated at 45 ºC for 4 h, and then the samples were boiled and analyzed with HPLC, on an Aminex-HPX-87P column (BioRad), with ultrapure water as eluent at a 0.6 mL min^{-1}, for a total of 30 min analysis. The column temperature was set at 85 ºC, and the injection volume was 5 µL.

Feruloyl esterase activity was measured in MOPS buffer pH 6, 100 mM against methyl ferulate 1 mM as substrate. Sodium azide was also added, at a final concentration of 1 mM, in order to avoid laccase-mediated oxidation of the substrate. The reaction was incubated at 40 ºC for 2h, and then the samples were boiled and analyzed with HPLC. The released ferulic acid was measured with a 1260 Infinity II HPLC system (Agilent Technologies), with a C18 CC 250/4.6 Nucleosil 100-5 column (Macherey-Nagel), and a UV-Vis 1260 Infinity II Variable Wavelength Detector, operating at 280 and 325 nm. The analysis was performed with 65 % (v/v) methanol as mobile phase, at 1 mL min^{-1}, and 40 ºC for 10 min.

For the aryl alcohol oxidase activity, a coupled assay was employed. Veratryl alcohol was used as substrate, at a final concentration of 5 mM, in a 100 mM phosphate buffer, pH 6. After crude enzyme addition, the mixture was incubated at 35 ºC for 15 min. Then, a mixture of 60 µg mL^{-1} HRP and 100 µg mL^{-1} phenol red were added, and the reaction was incubated for a further 5 min. Finally, the reaction was terminated by the addition of 1 N NaOH, and the absorbance was read at 610 nm. The produced H_2O_2 was quantified against a suitable calibration curve. Versatile peroxidase activity was measured as previously described (Camarero et al., 1999). 1 Unit of enzyme activity was defined as the enzyme quantity responsible for the release of 1 µmol product per min, under the assay conditions. Heat-denaturated samples were used as blanks in each case.

In order to test the hydrolytic potential of the secreted enzymes from *A. biennis* against LCB, the crude supernatant was concentrated 10 times with an ultrafiltration device (Amicon

chamber 8400 with membrane DiafloPM-10, exclusion size 10 kDa, Millipore, Billerica, USA). The retentate was added to two different pretreated samples, representative of different plant materials, namely beechwood (acetone:water oxidation pretreated, Acetone:H_2O, 50:50, $P_{O2,}$ initial 16 bar, 150 ^oC, for 60 min, composition: glucose 57.5 % (w/w), xylose, 22.6 % (w/w), and lignin 16.1 % (w/w) (Katsimpouras et al., 2017)) and corn stover (hydrothermally pretreated, with 0.3 % (v/v) acetic acid, 230 ^oC, 15 min, composition: glucose 47.1 % (w/w), xylose, 6.9 % (w/w), arabinose, 1.5 % (w/w) and lignin 32.4 % (w/w) (Katsimpouras et al., 2016)), at a final concentration of 50 mg mL^{-1}, in 100 mM phosphate buffer, pH 5.5. After 24 h incubation in 45 ^oC and 1200 rpm, the supernatants were collected and the reducing sugars were determined with the DNS method. Xylose, xylobiose and glucose were quantified with HPLC, as described above.

Text S2

2. Proteomic analysis

2.1 Sample preparation

For the secretome analysis, *A. biennis* was cultured as described in Section 2.1. After 14 days of growth in corn stover medium, the mycelia were removed by filtration, and the supernatant was ultrafiltrated and freeze-dried. Cultures of *A. biennis* in defined medium with xylose as carbon source were used as controls for the differential expression analysis. Protein extracts were dissolved in 5 % SDS in 50 mM triethyl ammonium bicarbonate (TEAB) to a final concentration of 1 μg $μl^{-1}$. To remove sugars, an aliquot from each sample containing 100 μg of protein was filtered with a 3 kDa Nanosep filter (Pall) according to the manufacturer's guidelines. Proteins retained on the filter membrane were re-dissolved in 300 μl 5 % SDS in 50 mM TEAB and reduced by addition of 15 mM DTT and incubation for 30 minutes at 55

°C followed by alkylation by addition of 30 mM iodoacetamide and incubation for 15 min in the dark. Phosphoric acid was added to a final concentration of 1.2 % to lower the pH to 1, followed by addition of 7 volumes of 90 % methanol in 100 mM TEAB at pH 7.55. Samples were loaded on mini S-trap columns (Protifi) in aliquots of 400 µl centrifuged each time for 30 seconds at 4000 xg, followed by 3 washing steps with 400 µl 90 % methanol in 100 mM TEAB. Then, 1 µg of MS-grade trypsin (Promega) in 125 µl 50 mM TEAB was added onto the filter and incubated overnight at 37 °C to digest the proteins. Finally, peptides were eluted from the S-trap columns in 3 centrifugation steps of 1 minute at 4000 x *g*, first with 80 µl 50 mM TEAB, then with 80 µl 0.2 % formic acid and finally with 80 µl 50 % acetonitrile. The eluted peptides were transferred into an MS vial, dried completely by vacuum drying and re-dissolved in 0.1% TFA in water/ACN (98:2, v/v)) for an additional purification step on Omix C18 tips (Agilent). The resulting purified peptides were dried completely by vacuum drying.

2.2 LC-MS/MS analysis

Peptides were re-dissolved in 20 µl loading solvent A (0.1 % TFA in water/ACN (98:2, v/v)) and firstly loaded on a trapping column (made in-house, 100 µm internal diameter (I.D.) × 20 mm, 5 µm beads C18 Reprosil-HD, Dr. Maisch, Ammerbuch-Entringen, Germany). Then, they were separated on a 50 cm µPAC™ GEN2 column and eluted by a stepped gradient from 98 % solvent A (0.1 % formic acid in water) to 30 % solvent B (0.1% formic acid in water/acetonitrile, 20/80 (v/v)) in 135 min up to 50 % MS solvent B in 15 min, followed by a 5 min wash reaching 95 % solvent B, all at a constant flow rate of 250 nL min^{-1}. The mass spectrometer (Ultimate 3000 RSLC nano- LC (Thermo Fisher Scientific, Bremen, Germany) in-line connected to a Q Exactive mass spectrometer (Thermo Fisher Scientific)) was operated in data-dependent, positive ionization mode, automatically switching between MS and MS/MS acquisition for the 5 most abundant peaks in a given MS spectrum. The source voltage was set to 3.0 kV, and the capillary temperature was 275 °C. One MS1 scan (m/z 400−2,000, AGC

target 3 ×E6 ions, maximum ion injection time 80 ms), acquired at a resolution of 70,000 (at 200 m/z), was followed by up to 5 tandem MS scans (resolution 17,500 at 200 m/z) of the most intense ions fulfilling predefined selection criteria (AGC target 50.000 ions, maximum ion injection time 80 ms, isolation window 2 Da, fixed first mass 140 m/z, spectrum data type: centroid, intensity threshold 1.3xE4, exclusion of unassigned, 1, 5-8, >8 positively charged precursors, peptide match preferred, exclude isotopes on, dynamic exclusion time 12 s). The HCD collision energy was set to 25 % Normalized Collision Energy and the polydimethylcyclosiloxane background ion at 445.120025 Da was used for internal calibration (lock mass). QCloud was used to control instrument longitudinal performance during the project (Chiva et al., 2018).

For the analysis of in-gel digested protein bands of *Abi*Lac1 and *Abi*Lac2, peptides were re-dissolved in 20 µl loading solvent A (0.1 % TFA in water/ACN (98:2, v/v)), and 5 µl were injected for LC-MS/MS analysis on an Ultimate 3000 RSLC nano- LC (Thermo Fisher Scientific, Bremen, Germany) in-line connected to a Q Exactive mass spectrometer (Thermo Fisher Scientific). Peptides were separated on a 50 cm µPAC™ GEN2 column with C18-endcapped functionality (Pharmafluidics, Belgium) kept at a constant temperature of 35 °C and eluted by a stepped gradient from 98 % solvent A (0.1 % formic acid in water) to 30 % solvent B (0.1 % formic acid in water/acetonitrile, 20/80 (v/v)) in 75 min up to 50 % MS solvent B in 25 min, followed by a 5 min wash reaching 99 % solvent B, all at a constant flow rate of 300 nL min^{-1}. The analysis was performed as described above using the intensity-based absolute quantification (iBAQ) algorithm (Schwanhäusser et al., 2011) instead of MaxLFQ for protein quantification. The raw spectral data files of both gel bands samples were searched separately and only proteins with at least one unique or razor peptide were retained.

2.3 Data analysis

The LC-MS/MS runs of all samples were searched together using MaxQuant v2.0.3.0 (Tyanova et al., 2016a) against the proteome of *A. biennis* CIRM-BRFM 1778 (v1.0, release date 2021-06-21, 11,767 sequences) (Hage et al., 2021) downloaded from MycoCosm (Grigoriev et al., 2014) and the MaxQuant common contaminant database. In addition, reversed sequences of all protein entries were concatenated to the database for estimation of false discovery rates (FDR). MaxQuant was run with default search settings, including, a false discovery rate set at 1 % on PSM, peptide and protein level. Protein identification and quantification was performed with the MaxLFQ workflow (Cox et al., 2014) using a minimum ratio count of 2 unique and razor peptides. Downstream processing was performed with Perseus v1.6.15.0 (Tyanova et al., 2016b) and the pandas Python package (https://zenodo.org/record/3715232#.YjGciDyxWrx and 10.25080/Majora-92bf1922-00a). The replicate samples were grouped into 'xylose' and 'corn stover' groups, LFQ protein intensities were Log2 transformed and only proteins found in at least two biological replicates of one group were kept for further analysis. Next, these proteins were filtered for extracellular proteins only, to exclude intracellular proteins released due to cell lysis during sample preparation.

Functional annotations of proteins including CAZymes, peptidases, signal peptides, InterPro domains, and KEGG classifications were downloaded from MycoCosm. For the identification of putative feruroyl esterases, we used BLASTp with 38 characterized fungal feruroyl esterases collected from Dilokpimol et. al., (Dilokpimol et al., 2016) against the proteome of *A. biennis* with the following criteria: >40 % protein sequence identity, and >70 % coverage of both sequences. Proteins were searched for the presence of transmembrane domains with TMHMM v2 (Krogh et al., 2001) and their subcellular localization was predicted with the DeepLoc algorithm (Almagro Armenteros et al., 2017). The extracellular

dataset contains proteins classified as extracellular with DeepLoc and proteins that possess signal peptides and have no transmembrane helices in the mature protein.

For the comparison of protein abundances between the two groups, proteins detected in at least two samples of corn stover and one sample of xylose were considered. Their missing LFQ intensities were imputed from a normal distribution with 0.3 spread and 1.8 downshift with Perseus. Protein LFQ intensities were tested using a two-sided Student‘s t-test with a permutation-based false discovery rate of 5 % and 250 randomizations.

Text S3

3. Protein analysis of AbiLac1 and AbiLac2

The bands were washed by vortexing in 100 µl water and incubated for 15 minutes at room temperature, followed by a second wash in 100 µl 50:50 (v/v) acetonitrile/water and a third wash in 100 µl acetonitrile. The supernatant was discarded and gel bands were dried completely by vacuum drying. Gel bands were re-hydrated by absorption of 15 µl of a digestion solution containing 0.005 µg MS-grade trypsin (Promega) in 50 mM ammonium bicarbonate after which 50 µl 50 mM ammonium bicarbonate was added until the bands were fully submerged and samples were incubated overnight at 37 °C. The next day, the peptide mixture eluted from the gel was acidified with 2 µl formic acid, transferred to an MS vial and dried completely by vacuum drying.

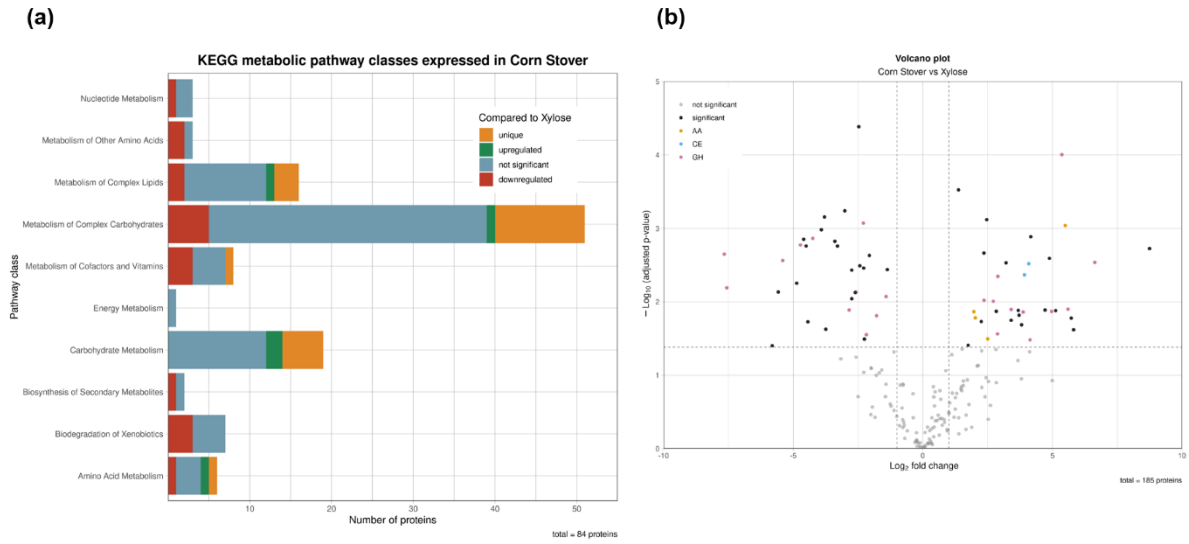

Fig. S1. (a) KEGG classification of the detected proteins in *A. biennis* secretomes, after growth in corn stover (b) Volcano plot with the differential expression of proteins found in both growth conditions.

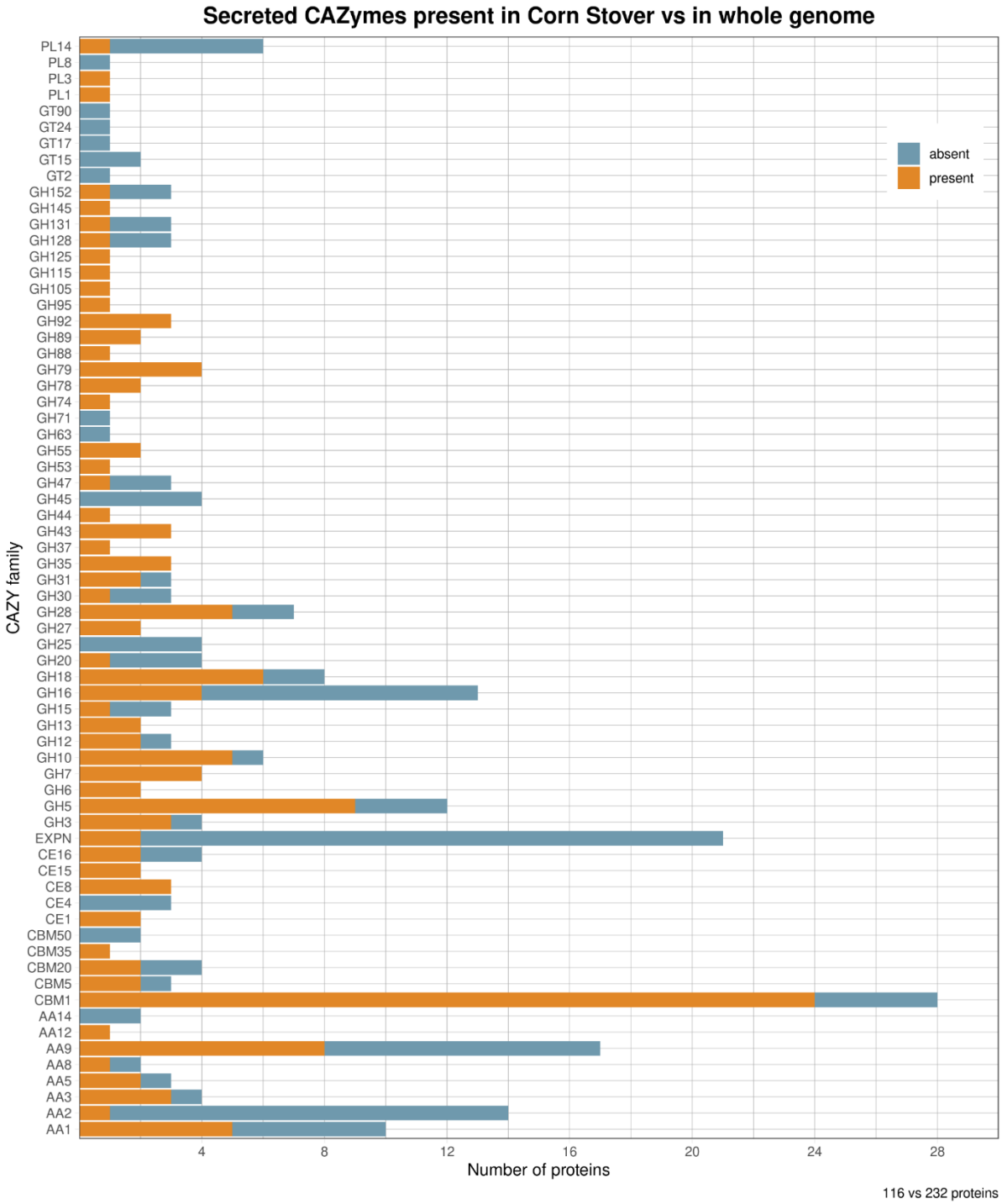

Fig. S2. CAZymes detected in *A. biennis* secretomes, when grown in corn stover cultures, compared to the predicted CAZymes present in the genome.

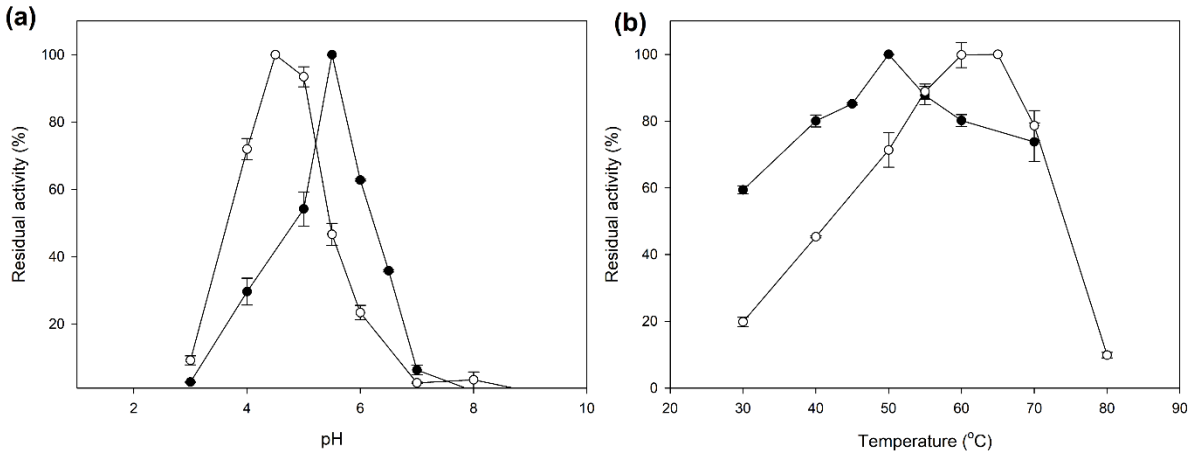

Fig. S3. pH (a) and temperature (b) dependence of purified *Abi*Lac1 (*black circles*) and *Abi*Lac2 (*white circles*).

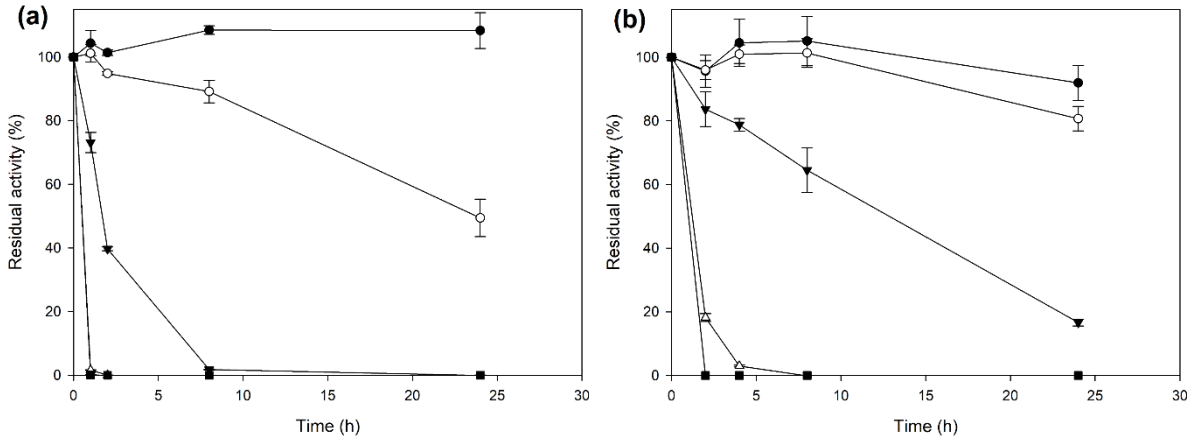

Fig. S4. Thermostability of purified *Abi*Lac1 (a) and *Abi*Lac2 (b), at 30 ºC (*black circles*) 40 ºC, (*white circles*), 50 ºC (*black inverted triangles*), 60 ºC (*white triangles*) and 70 ºC (*black squares*).

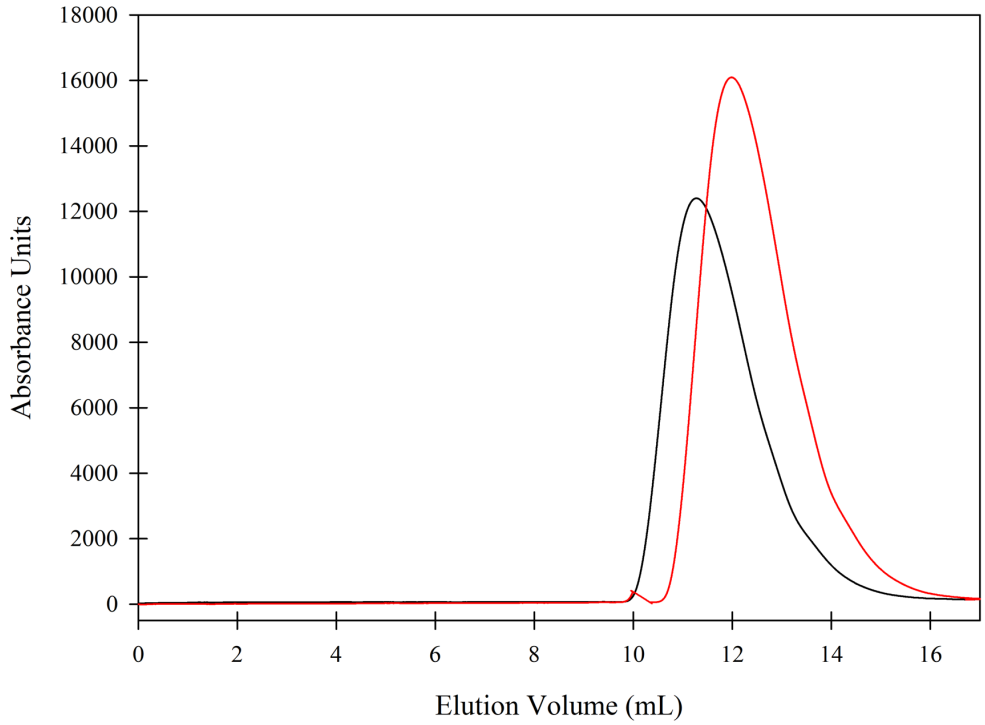

Fig. S5. Molecular weight determination of control sample (*black line*) and enzymatically treated sample (*red line*).

Table S1. Purification of *Abi*Lac1 and *Abi*Lac2 from the culture supernatant of *A. biennis*

Substrate	***Abi*Lac1**			***Abi*Lac2**		
	Specific activity (U mg^{-1})	Purification (fold)	Yield (%)	Specific activity (U mg^{-1})	Purification (fold)	Yield (%)
Crude	0.38	1	100	0.38	1	100
Q-sepharose	4.76	12.59	12.9	2.03	5.37	4.14

Table S2. Substrate oxidation spectrum of *Abi*Lac1 and *Abi*Lac2. Activity, in terms of absorbance difference in the recorded UV/Vis spectrum between reaction and blank, is indicated with (+) when positive (indicating absorbance difference in the spectrum maxima), with (−) when negative and with (±) when ambiguous. Multiple (+) signs indicate differences higher than 1 (++) or 2 (+++) absorbance units

a/a	Substrate	*Abi*Lac1	*Abi*Lac2
Hydroxybenzoles			
1	Phenol	-	±
2	Catechol	+++	+++
3	Resorcinol	+++	+++
4	Hydroquinone	+++	+++
5	Chlorocatechol	+++	+++
6	Pyrogallol	+++	+++
Methoxyphenols			
7	Guaiacol	+++	++
8	2,6-dimethoxyphenol	+	+
Aromatic alcohols			
9	3,4-dimethoxybenzyl alcohol	±	±

Aromatic amines			
10	Aniline	±	±
Phenolic aldehydes			
11	Vanillin	+	+
Flavonoids			
12	Quercetin	+++	+++
13	Catechin	+++	+++
Hydroxycinnamic acids			
14	Caffeic acid	+	+
15	Ferulic acid	+	+
16	Sinapic acid	++	++
17	*p*-coumaric acid	++	++
Hydroxybenzoic acids			
18	Vanillic acid	+++	+++
19	Gallic acid	+++	+++
20	*p*-hydroxybenzoic acid	-	±
21	Protocatechuic acid	+++	+++
Aromatic azo-compounds			
22	ABTS	+++	+++
Other acids			
23	Ascorbic acid	+++	+++
Cresols			
24	*o*-cresol	-	±
25	*m*-cresol	±	±
26	*p*-cresol	+	+

Table S3. Substrate specificity of *Abi*Lac1 and *Abi*Lac2

Substrate	*Abi*Lac1 (Units mg^{-1})	*Abi*Lac2 (Units mg^{-1})
ABTS	61.0 ± 1.0	31.0 ± 1.0
Catechol	43.6 ± 0.4	16.1 ± 0.2
2,6-DMP	24.0 ± 1.0	13.0 ± 2.0
Guaiacol	15.7 ± 0.1	7.1 ± 0.2
Pyrogallol	10.7 ± 0.4	5.9 ± 0.1

Table S4. Michaelis–Menten kinetic parameters for *Abi*Lac1 and *Abi*Lac2 in ABTS and catechol

Substrate	*Abi*Lac1		*Abi*Lac2	
	ABTS	Catechol	ABTS	Catechol
K_m (mM)	0.05 ± 0.005	2.57 ± 0.086	0.02 ± 0.002	0.94 ± 0.043
k_{cat} (1/min)	2036.63 ± 56.555	4050.90 ± 49.228	575.89 ± 12.362	1031.80 ± 17.087
k_{cat}/K_m (1/μM*min)	39.98 ± 3.926	1.58 ± 0.057	26.38 ± 2.641	1.10 ± 0.053

Table S5. Weight loss and molecular weight decrease after treating PS with purified *Abi*Lac1

	% weight loss	% $\overline{M_w}$ decrease	% $\overline{M_n}$ decrease	PDI
Control	1.2 ± 0.6	0	0	1.9
Enzymatically treated PS	6.4 ± 0.7	7.7 ± 1.5	19.7 ± 2.9	2.2

References

Almagro Armenteros, J.J., Sønderby, C.K., Sønderby, S.K., Nielsen, H., Winther, O., 2017. DeepLoc: prediction of protein subcellular localization using deep learning. Bioinformatics 33, 3387–

3395. https://doi.org/10.1093/bioinformatics/btx431

Camarero, S., Sarkar, S., Ruiz-Dueñas, F.J., Martínez, M.J., Martínez, Á.T., 1999. Description of a Versatile Peroxidase Involved in the Natural Degradation of Lignin That Has Both Manganese Peroxidase and Lignin Peroxidase Substrate Interaction Sites. J. Biol. Chem. 274, 10324–10330. https://doi.org/10.1074/jbc.274.15.10324

Chiva, C., Olivella, R., Borràs, E., Espadas, G., Pastor, O., Solé, A., Sabidó, E., 2018. QCloud: A cloud-based quality control system for mass spectrometry-based proteomics laboratories. PLoS One 13, e0189209. https://doi.org/10.1371/journal.pone.0189209

Cox, J., Hein, M.Y., Luber, C.A., Paron, I., Nagaraj, N., Mann, M., 2014. Accurate Proteome-wide Label-free Quantification by Delayed Normalization and Maximal Peptide Ratio Extraction, Termed MaxLFQ. Mol. Cell. Proteomics 13, 2513–2526. https://doi.org/10.1074/mcp.M113.031591

Dilokpimol, A., Makela, M.R., Aguilar-Pontes, M. V, Benoit-Gelber, I., Hilden, K.S., de Vries, R.P., 2016. Diversity of fungal feruloyl esterases: updated phylogenetic classification, properties, and industrial applications. Biotechnol Biofuels 9, 231. https://doi.org/10.1186/s13068-016-0651-6

Grigoriev, I. V., Nikitin, R., Haridas, S., Kuo, A., Ohm, R., Otillar, R., Riley, R., Salamov, A., Zhao, X., Korzeniewski, F., Smirnova, T., Nordberg, H., Dubchak, I., Shabalov, I., 2014. MycoCosm portal: gearing up for 1000 fungal genomes. Nucleic Acids Res. 42, D699–D704. https://doi.org/10.1093/nar/gkt1183

Hage, H., Miyauchi, S., Virágh, M., Drula, E., Min, B., Chaduli, D., Navarro, D., Favel, A., Norest, M., Lesage-Meessen, L., Bálint, B., Merényi, Z., Eugenio, L., Morin, E., Martínez, A.T., Baldrian, P., Štursová, M., Martínez, M.J., Novotny, C., Magnuson, J.K., Spatafora, J.W., Maurice, S., Pangilinan, J., Andreopoulos, W., LaButti, K., Hundley, H., Na, H., Kuo, A., Barry, K., Lipzen, A., Henrissat, B., Riley, R., Ahrendt, S., Nagy, L.G., Grigoriev, I. V., Martin, F., Rosso, M., 2021. Gene family expansions and transcriptome signatures uncover fungal adaptations to wood decay. Environ. Microbiol. 23, 5716–5732. https://doi.org/10.1111/1462-2920.15423

Katsimpouras, C., Christakopoulos, P., Topakas, E., 2016. Acetic acid-catalyzed hydrothermal pretreatment of corn stover for the production of bioethanol at high-solids content. Bioprocess Biosyst. Eng. 39, 1415–1423. https://doi.org/10.1007/s00449-016-1618-5

Katsimpouras, C., Kalogiannis, K.G., Kalogianni, A., Lappas, A.A., Topakas, E., 2017. Production of high concentrated cellulosic ethanol by acetone/water oxidized pretreated beech wood. Biotechnol. Biofuels 10, 54. https://doi.org/10.1186/s13068-017-0737-9

Krogh, A., Larsson, B., von Heijne, G., Sonnhammer, E.L.., 2001. Predicting transmembrane protein topology with a hidden markov model: application to complete genomes11Edited by F. Cohen. J. Mol. Biol. 305, 567–580. https://doi.org/10.1006/jmbi.2000.4315

Miller, G.L., 1959. Use of Dinitrosalicylic Acid Reagent for Determination of Reducing Sugar. Anal. Chem. 31, 426–428. https://doi.org/10.1021/AC60147A030/ASSET/AC60147A030.FP.PNG_V03

Schwanhäusser, B., Busse, D., Li, N., Dittmar, G., Schuchhardt, J., Wolf, J., Chen, W., Selbach, M., 2011. Global quantification of mammalian gene expression control. Nature 473, 337–342. https://doi.org/10.1038/nature10098

Tyanova, S., Temu, T., Cox, J., 2016a. The MaxQuant computational platform for mass spectrometry-based shotgun proteomics. Nat. Protoc. 11, 2301–2319. https://doi.org/10.1038/nprot.2016.136

Tyanova, S., Temu, T., Sinitcyn, P., Carlson, A., Hein, M.Y., Geiger, T., Mann, M., Cox, J., 2016b. The Perseus computational platform for comprehensive analysis of (prote)omics data. Nat.

Methods 13, 731–740. https://doi.org/10.1038/nmeth.3901

Zerva, A., Koutroufini, E., Kostopoulou, I., Detsi, A., Topakas, E., 2019. A novel thermophilic laccase-like multicopper oxidase from Thermothelomyces thermophila and its application in the oxidative cyclization of 2′,3,4-trihydroxychalcone. N. Biotechnol. 49. https://doi.org/10.1016/j.nbt.2018.12.001

Zerva, A., Savvides, A.L., Katsifas, E.A., Karagouni, A.D., Hatzinikolaou, D.G., 2014. Evaluation of Paecilomyces variotii potential in bioethanol production from lignocellulose through consolidated bioprocessing. Bioresour. Technol. 162. https://doi.org/10.1016/j.biortech.2014.03.137